ELSEVIER

Biophysical Chemistry 104 (2003) 393–405

Biophysical Chemistry

www.elsevier.com/locate/bpc

# On the cavity size distribution in water and *n*-hexane

Giuseppe Graziano*

*Dipartimento di Scienze Biologiche e Ambientali, Facoltà di Scienze, Università del Sannio, Via Port'Arsa, 11-82100 Benevento, Italy*

Received 29 October 2002; received in revised form 17 January 2003; accepted 17 January 2003

**Abstract**

The cavity size distribution functions in water and *n*-hexane were determined by Pohorille and Pratt, in a series of important works, from molecular dynamics simulations. These functions are considered as experimental data. In the present investigation the ability of scaled particle theory in reproducing such distributions is tested. In the case of water the scaled particle theory results compare favorably with the experimental distribution if a proper choice of the size to be assigned to water molecules is performed. Specifically, a slight size increase from 2.70 to 2.80 Å is necessary to reach agreement for the largest cavities detected by Pohorille and Pratt. In the case of *n*-hexane the scaled particle theory results do not agree with the experimental distribution especially in the region of small cavities. This deficiency is because a *n*-hexane molecule cannot be realistically treated as a single spherical exclusion volume. The implications of such findings are analyzed and discussed in depth.


*Keywords:* Cavity size distribution; Scaled particle theory; Molecular size

## 1. Introduction

A simple physical argument suggests that the free volume in a liquid should be distributed in smaller or larger packets depending on the size of liquid molecules, because the latter is the characteristic length-scale of the liquid itself [1]. This idea, coupled with the scaled particle theory (SPT) results for the work of cavity creation in different liquids [2,3], led to an interesting conclusion. Hydrophobicity, the poor solubility of non-polar compounds in liquid water, should be mainly due to the very small size of water molecules and only indirectly to the existence of the H-bonding network [1,4–10]. Consider that the size of a water molecule, corresponding practically to that of an oxygen atom, is the smallest one among all common solvents.

Pohorille and Pratt [11–13], (P&P), decided to test this idea directly, by performing molecular dynamics (MD) computer simulations of several liquids and determining the cavity size distribution in each one (actually we shall limit our analysis to water and *n*-hexane). They took a first significant step and a further evolution of these calculations and concepts has occurred over the intervening decade [14–22]. The water molecules were treated as single spherical exclusion volumes of 2.70 Å diameter, and the methyl and methylene

*Corresponding author. Tel.: +39-0824-305101; fax: +39-0824-23013.

*E-mail address:* graziano@unisannio.it (G. Graziano).

0301-4622/03/$ - see front matter 
doi:10.1016/S0301-4622(03)00027-9

groups of *n*-hexane as united atom spherical exclusion volumes of 3.70 Å diameter [11]. P&P created a grid of test points evenly spaced in the simulation box and determined, for each liquid configuration and each grid-point, the nearest exclusion sphere. This procedure allowed the determination of the radius of the largest cavity that could be inserted at the grid-point in question for that particular liquid configuration. [Note that there are two measures of the cavity size [23]: (a) the radius of the spherical region from which all parts of the solvent molecules are excluded, indicated by $r_c$; (b) the radius of the spherical region from which the centers of the solvent molecules are excluded, indicated by $R_c$. In the case of spherical particles, the following relation holds: $R_c = r_c + r_1$, where $r_1$ is the radius of the solvent molecules. Both measures are used in the present work, but it is worth noting that $r_c$ has to be used when comparing cavity distributions in different liquids.] The radii of the largest cavities that could be inserted were binned and averaged over both grid-points and sampled configurations. In this manner P&P calculated the probability density of the radius of the largest cavity that could be successfully inserted, $P_{max}(r_c)$.

The two functions determined by P&P [11–13] are shown in Fig. 1, including the range of negative $r_c$ where they are non-zero (i.e. the lower limit of their natural range is $r_c = -r_1$). These distributions have to be considered as 'experimental' data. The Hertz distribution [24], valid when the molecules are randomly distributed as in an ideal gas, is also shown in Fig. 1, by considering the same number density of liquid water at 300 K and the same size of water molecules [13]. The maximum of the cavity size distribution function represents the most probable value of the cavity radius that could be inserted into the liquid. P&P pointed out that such maximum occurs at $r_c \cong 0.2$ Å in both water and *n*-hexane and it is higher for water [11–13]. Very small cavities (i.e. $r_c < 0.7$ Å) are more probable in water than in *n*-hexane, because the free volume is larger for water than for common organic solvents, reminiscent of the open structure of ice.

In addition, such maximum occurs at a size significantly less than that for the Hertz random distribution, $r_c \cong 0.35$ Å. P&P [13] pointed out

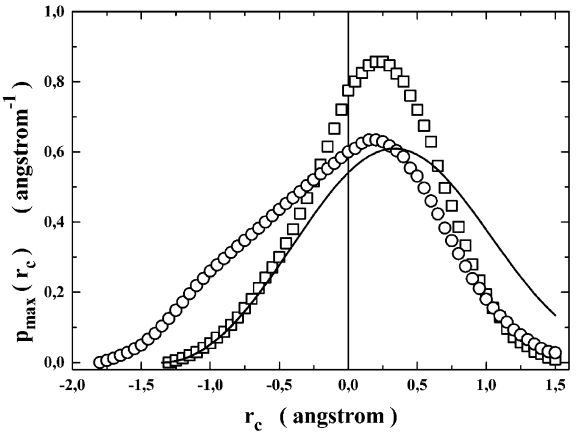


Fig. 1. Cavity size distribution functions for TIP4P water at 300 K (empty squares), and for an OPLS model of *n*-hexane at 320 K (empty circles), determined by P&P from the analysis of MD computer simulations [11–13]. They have to be considered as 'experimental' data. The Hertz distribution [24], $P_{max}(r_c) = 4\pi \cdot \rho_1 \cdot (r_c + r_1)^2 \cdot \exp[-4\pi \cdot \rho_1 \cdot (r_c + r_1)^3/3]$, valid when the molecules are randomly distributed, is also shown as a continuous line, for the case having the same number density and the same molecular size of liquid water.

that: 'The interpretation is that cavities of larger size are formed by fluctuations that compress the fluid in some regions in order to rarify it in other regions. The random distribution does not account for excluded volume interactions between the solvent molecules and such fluctuations happen with higher probability for the random distribution of atom centers than for distributions encountered in real solvents.' This finding emphasizes the fundamental role played by the repulsive part of the intermolecular potential in liquids (i.e. each molecule possesses a hard core impenetrable to the others) [25].

Clearly, if the most probable value of $r_c$ were taken as the unique indicator of the size of typical cavities occurring in these two liquids, one should conclude that there is no important difference between the cavity sizes characterizing water and *n*-hexane. However, the width of the $P_{max}(r_c)$ distribution function is the fundamental quantity since molecular-sized cavities (i.e. those having a diameter of few angstroms are important for the solvation of real solutes) occur in the positive tail of the distribution. According to the P&P results

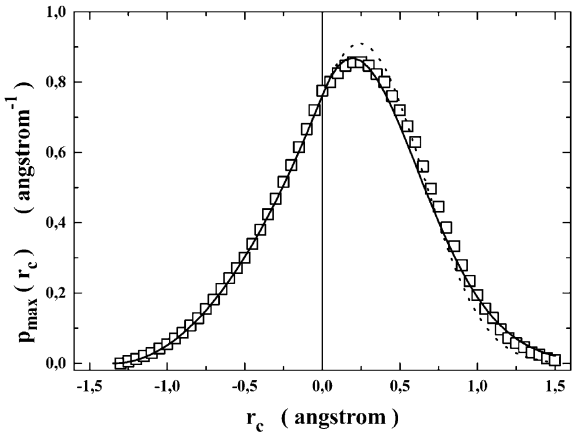


Fig. 2. Comparison between the 'experimental' cavity size distribution for water (empty squares), and those calculated using Eqs. (11) and (13) for $\sigma_1 = 2.70$ Å, and $P = 1$ atm (solid line); and $\sigma_1 = 2.70$ Å and $P = P(\mathrm{SPT}) = 7000$ atm (dotted line). The experimental density of water at 300 K is used in both cases.

[11–13], the width of the $P_{\max}(r_c)$ distribution function is significantly larger for *n*-hexane than for water: the two distributions cross each other at $r_c \cong 1.1$ Å (see Fig. 1). In this respect, it should be noted that [12]: (a) the widths of these distributions are independent of the diameters assigned to solvent molecules; (b) 'the relative narrowness of $P_{\max}(r_c)$ is a distinctive feature of liquid water.' This means that it is more and more probable to find a molecular-sized cavity in *n*-hexane than in water. Therefore, it seems to validate the physical argument that the free volume is partitioned in smaller cavities in water than in common organic solvents due to the relatively small size of water molecules.

Actually, P&P provided a different explanation [11–13]: water is stiffer than common organic solvents when molecular-sized cavities have to be opened due to the presence of H-bonds. To arrive at such a conclusion they determined the contact correlation function for both solvents, obtaining that this quantity is markedly larger for water than for *n*-hexane. This implies that 'water applies more force per unit area of cavity surface than do hydrocarbon liquids' [12]. In addition, P&P pointed out the SPT failure to quantitatively reproduce the values of $\Delta G_c$ determined from their computer simulations of liquid water [11]. Thus, P&P concluded that a hard sphere fluid, having the same density of liquid water and whose molecules have the same size of those of water, finds more ways to distribute its free volume into packets of sufficiently large size to accommodate the solute with respect to liquid water [11,12]. This would be a simple consequence of the fundamental role played by the H-bonding network in liquid water.

The width of the $P_{\max}(r_c)$ distribution function is an intrinsic property of each liquid and it is important to try to establish which physical features of the liquid determine it. To this aim, in the present work, we test the ability of SPT, an analytical theory originally developed for hard sphere fluids [2], to reproduce the cavity size distributions determined by P&P for water and *n*-hexane.

## 2. Theory

### 2.1. General relationships

According to the statistical mechanical theory of fluctuations [26], the probability of finding a spherical region of radius $R_c$ devoid of solvent molecule centers, at an arbitrarily fixed position, is related to the reversible work required to produce such constrained molecular configuration starting from the equilibrium one:

$$P_0(R_c) = \exp[-W(R_c)/RT] \tag{1}$$

If the system is at constant temperature and pressure, the reversible work corresponds to the Gibbs energy change associated with cavity creation, $W(R_c) = \Delta G_c(R_c)$, so that:

$$\Delta G_c(R_c) = -RT \cdot \ln P_0(R_c) \tag{2}$$

Note that $\Delta G_c$ is a positive quantity also to create a point cavity at a fixed position (i.e. $r_c = 0$ implies $R_c = r_1$), because, even though such a cavity has a van der Waals surface area of zero, it gives rise to a non-zero solvent excluded volume of $(4/3)\pi \cdot r_1^3$.

Simple geometric considerations lead to the following relationship [27,28]:

$$P_0(R_c) = \langle V_{avail}(R_c) \rangle / V_{tot} \quad (3)$$

where the ratio is the fraction of the total volume containing cavities whose radius is at least equal to $R_c$, and the brackets represent an ensemble average value. The quantity $P_0$ is also called the cavity insertion probability [11]. The combination of Eqs. (2) and (3) indicates that $\Delta G_c$ can be calculated by directly determining the molecular-scale density fluctuations of a liquid model by means of computer simulations [11,27].

Reiss and colleagues [29,30] showed that: (a) the cavity insertion probability $P_0$ depends only on $R_c$, not on $r_c$ or $r_1$ separately; (b) it can be expressed by means of a function $h(R)$, related to the nearest neighbor distribution function [24]. Specifically, $h(R)dR$ is the probability that the distance of the center of the nearest neighbor spherical molecule from an arbitrary point in the liquid is in the range $R$ to $R+dR$. In general, the probability of the desired event is given by the certainty minus the probability of the undesired event, so that:

$$P_0(R_c) = 1 - \int_0^{R_c} h(R)dR \quad (4)$$

where the integral represents the probability that the center of at least one solvent molecule is in the spherical region of radius $R_c$ (i.e. the probability of the undesired event). It is worth noting that, on the basis of the definition of $R_c$, $R_c = 0$ means $r_c = -r_1$, a cavity with a negative radius, equal in size to that of solvent molecules (i.e. a negative cavity radius is physically meaningful, but it cannot be smaller than the above limit).

Actually, by changing the point of view, $P_0(R_c)$ is also given by:

$$P_0(R_c) = \int_{R_c}^{\infty} h(R)dR \quad (5)$$

where the integral represents the probability that the distance of the center of the nearest neighbor spherical molecule from an arbitrary point in the liquid is between $R_c$ and $\infty$ (i.e. not smaller than $R_c$). In other words, the integral exactly represents the probability that a cavity of radius at least equal to $R_c$ does exist in the liquid. This means that the function $h(R)$ corresponds also to the probability density of the radius of the largest cavity that can be successfully inserted in the liquid, indicated as $P_{max}(R)$. The latter function has to be interpreted by considering that $P_{max}(R)dR$ is the probability that the radius of the largest cavity that can be inserted is in the range $R$ to $R+dR$. Therefore, $P_{max}(R)$ is the cavity size distribution in the liquid, and Eq. (5) can be re-written as:

$$P_0(R_c) = \int_{R_c}^{\infty} P_{max}(R)dR \quad (6)$$

By differentiating both sides of Eq. (6) with respect to the cavity radius $r_c$ (consider that $r_1$, the radius of solvent molecules, is a constant quantity), one obtains:

$$P_{max}(r_c) = -(\partial P_0 / \partial r_c) \quad (7)$$

Therefore, the negative derivative of the insertion probability with respect to the cavity radius gives the cavity size distribution in the liquid [11,12]. This relationship clarifies that the cavity size distribution in a liquid, $P_{max}(r_c)$, can be calculated from the cavity insertion probability, $P_0(R_c)$, that is related to $\Delta G_c$ by means of Eqs. (1) and (2).

Another key quantity, the contact correlation function $G(R_c)$, which is the conditional solvent density just outside a spherical cavity of radius $R_c$ [2], is given by:

$$G(R_c) = -(1/4\pi \cdot \rho_1 \cdot R_c^2) \cdot (d\ln P_0 / dR_c) = (1/4\pi \cdot \rho_1 \cdot R_c^2) \cdot (P_{max}/P_0) \quad (8)$$

where the second equality comes directly from Eq. (7). The following general relation connects $G(R_c)$ to the work of cavity creation:

$$W(R_c) = RT \cdot 4\pi \cdot \rho_1 \int_0^{R_c} R^2 \cdot G(R)dR \quad (9)$$

where $RT$ is the thermal energy, and the quantity $RT \cdot 4\pi \cdot \rho_1 \cdot R_c^2 \cdot G(R_c)$ can be viewed as the compressive force exerted by the solvent molecules on the cavity whose surface area is $4\pi R_c^2$ [2,12].

### 2.2. Application of SPT

Reiss and colleagues [28–30] pointed out that simple geometric arguments lead to the following exact relationship for $R_c \leq r_1$ (i.e. at most one molecular center can be found in the cavity for $0 \leq R_c \leq r_1$):

$$\Delta G_c = -RT \cdot \ln[1-(4/3)\pi \cdot \rho_1 \cdot R_c^3] \quad (10)$$

where $\rho_1 = N_{Av}/v_1$ is the number density of the solvent and $v_1$ its molar volume. Application of Eqs. (2) and (7) gives:

$$P_{max}(-r_1 \leq r_c \leq 0) = 4\pi \cdot \rho_1 \cdot R_c^2 \quad (11)$$

When $R_c \geq r_1$, SPT provided the following formula for $\Delta G_c$ [3]:

$$\Delta G_c = RT \cdot [K_0 + K_1(\sigma_c/\sigma_1) + K_2(\sigma_c/\sigma_1)^2 + K_3(\sigma_c/\sigma_1)^3] \quad (12)$$

where: $K_0 = -\ln(1-\xi)$; $K_1 = u = 3\xi/(1-\xi)$; $K_2 = u\ (u+2)/2$; $K_3 = \xi \cdot P \cdot v_1/RT$. In these relations $R$ is the gas constant; $\xi$ is the volume packing density of pure solvent, which is defined as the ratio of the physical volume of a mole of solvent molecules over the molar volume of the solvent (i.e. $\xi = \pi \cdot \sigma_1^3 \cdot N_{Av}/6 \cdot v_1$); $\sigma_c$ and $\sigma_1$ are the hard sphere diameter of the cavity and of the solvent molecules, respectively; and $P$ is the pressure. On the basis of Eqs. (2), (7) and (12) one obtains:

$$P_{max}(r_c \geq 0) = 2[(K_1/\sigma_1) + (2K_2/\sigma_1^2)\sigma_c + (3K_3/\sigma_1^3)\sigma_c^2] \cdot \exp(-\Delta G_c/RT) \quad (13)$$

We will use Eqs. (11) and (13) to try to reproduce the $P_{max}(r_c)$ distributions determined by P&P for TIP4P water [31] at 300 K, and for an OPLS model of *n*-hexane [32] at 320 K. This is important to further test the reliability of SPT in studying solvation thermodynamics in both water and organic solvents, first showed by Pierotti in the middle sixties [33,34]. In fact, both Ben–Naim and Friedman [35], and Stillinger [36] identified a specific flaw in SPT: the temperature dependence of the surface tension obtained for water is improper, even though its magnitude is reasonable. Pierotti [37], however, pointed out that the surface tension given by SPT refers to the interface between the liquid and a rigid plane wall, whereas ordinary surface tension measurements refer to the interface between the liquid and a dilute gas. It is a distinctive assumption to consider that these two surface tensions should not be different and should have the same temperature dependence.

To test the effect of pressure in Eqs. (12) and (13), values of the hard sphere pressure have been calculated by means of the SPT equation of state [2]:

$$P = (6kT/\pi\sigma_1^3) \cdot [\xi(1+\xi+\xi^2)/(1-\xi)^3] \quad (14)$$

where $k$ is the Boltzmann constant; they will be indicated as $P$(SPT) in the following.

According to Eqs. (8), (11) and (13), the contact correlation function $G(R_c)$ is given by:

$$G(0 \leq R_c \leq r_1) = 1/[1-(4/3)\pi \cdot \rho_1 \cdot R_c^3] \quad (15)$$

$$G(R_c \geq r_1) = (1/2\pi \cdot \rho_1 \cdot R_c^2) \cdot [(K_1/\sigma_1) + (2K_2/\sigma_1^2)\sigma_c] \quad (16)$$

where the $\sigma_c^2$ term has been neglected in Eq. (16) for its smallness when $P = 1$ atm. These two relationships will be used to try to reproduce the $G(R_c)$ function determined by P&P for TIP4P water at 300 K [12]. In this respect, it has to be noted that Stillinger [36] proposed revised SPT relationships for $G(R_c)$ by taking into account: (a) the experimental oxygen–oxygen radial distribution function of water; (b) the experimental surface tension of water. Even though the Stillinger's improved SPT seems to work well [38,39], we preferred to use the original SPT in order to perform a complete test of its reliability.

Finally, we would like to attach a clear meaning to the expression 'molecular-sized cavities' used

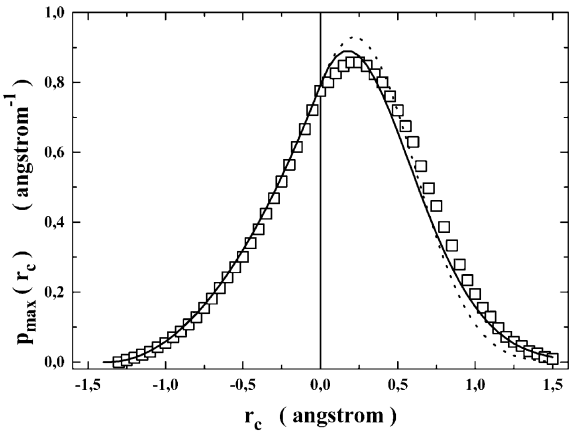


Fig. 3. Comparison between the 'experimental' cavity size distribution for water (empty squares), and those calculated using Eqs. (11) and (13) for $\sigma_1 = 2.75$ Å, and $P = 1$ atm (solid line); and $\sigma_1 = 2.75$ Å and $P = P(\mathrm{SPT}) = 7880$ atm (dotted line). The experimental density of water at 300 K is used in both cases.

in the following. Recently, Lum, Chandler and Weeks [40] developed a theory showing that there is a crossover between the work of cavity creation for small and large length scales due to drying of the cavity surface by the solvent molecules when the cavity radius exceeds a certain value. According to the Lum–Chandler–Weeks theory [40], the crossover occurs on the nanometer size range in liquid water. Thus, molecular-sized cavities in water are cavities of the size of a water molecule but also cavities suitable to host neopentane or benzene molecules (cavities of 5–6 Å diameter). At least the same should be true for *n*-hexane, since the drying mechanism is related to the strength of attractive interactions between solvent molecules.

## 3. Results

### *3.1. Water*

The cavity size distribution functions calculated for water using Eqs. (11) and (13) are contrasted against the 'experimental' one determined by P&P for TIP4P water at 300 K from MD simulations in Figs. 2–4. Specifically: (a) the $P_{max}(r_c)$ functions calculated for $\sigma_1 = 2.70$ Å and $P = 1$ atm (solid line), and $\sigma_1 = 2.70$ Å and $P = P(\mathrm{SPT}) = 7000$ atm (dotted line) are shown in Fig. 2; (b) the $P_{max}(r_c)$ functions calculated for $\sigma_1 = 2.75$ Å and $P = 1$ atm (solid line), and $\sigma_1 = 2.75$ Å and $P = P(\mathrm{SPT}) = 7880$ atm (dotted line) are shown in Fig. 3; (c) the $P_{max}(r_c)$ functions calculated for $\sigma_1 = 2.80$ Å and $P = 1$ atm (solid line), and $\sigma_1 = 2.80$ Å and $P = P(\mathrm{SPT}) = 8880$ atm (dotted line) are shown in Fig. 4. In all cases the experimental molar volume of water at 300 K, 18.07 cm$^3$ mol$^{-1}$, is used [41].

It is evident that all the $P_{max}(r_c)$ functions calculated using the pressure obtained from the SPT equation of state do not agree with the 'experimental' one. This may be considered a demonstration that $P$ has to be 1 atm in performing SPT calculations of $\Delta G_c$, as already claimed by several authors [3,36,42].

More important, the $P_{max}(r_c)$ function calculated for $\sigma_1 = 2.70$ Å and $P = 1$ atm is in reasonable agreement with the 'experimental' one up to $r_c \cong 1.1$ Å. Beyond this size, it tends to overestimate the probability of cavity occurrence. On the other hand, both the $P_{max}(r_c)$ functions calculated for $\sigma_1 = 2.75$ Å and 2.80 Å ($P = 1$ atm in both cases) do not agree with the 'experimental' one up to $r_c \approx 1.2$ Å, but the agreement becomes better

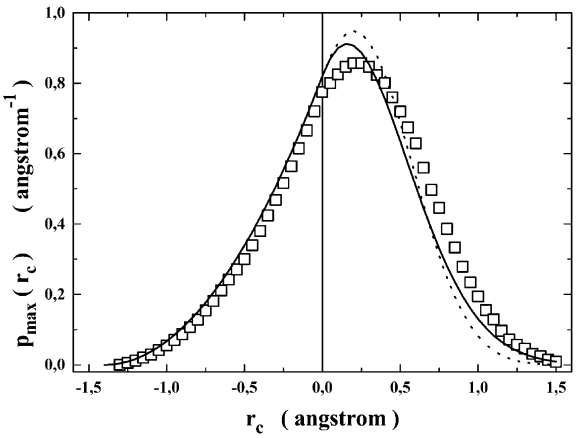


Fig. 4. Comparison between the 'experimental' cavity size distribution for water (empty squares), and those calculated using Eqs. (11) and (13) for $\sigma_1 = 2.80$ Å, and $P = 1$ atm (solid line); and $\sigma_1 = 2.80$ Å and $P = P(\mathrm{SPT}) = 8880$ atm (dotted line). The experimental density of water at 300 K is used in both cases.

and better on further increasing the cavity size (i.e. for molecular-sized cavities).

Since P&P assigned to each water molecule a hard sphere diameter of 2.70 Å [11–13], the above SPT results are understandable. For very small interstitial holes ($r_c \leq 1$ Å) the water molecule size selected by P&P is the controlling factor and SPT reproduces the experimental trend using the same $\sigma_1$ value (i.e. 2.70 Å). On increasing the cavity size beyond $r_c \approx 1$ Å, the diameter selected by P&P becomes less important in view of the procedure they adopted to determine $P_{max}(r_c)$. Note that, by a simple translation of solely $-0.05$ Å of the $r_c$ axis, the $P_{max}$ distribution obtained for $\sigma_1 =$ 2.70 Å is converted in that valid for $\sigma_1 = 2.80$ Å.

In contrast, SPT is extremely sensitive to the $\sigma_1$ value used because the latter quantity enters the formulas raised to various powers [2,3]. Therefore, SPT is able to provide satisfactory results for real liquids if and only if the $\sigma_1$ value is properly chosen. In this respect one has to consider that $\sigma_1 = 2.80$ Å is not an absurd value for the size of a water molecule, but a physically sound one according to the location of the first peak in the oxygen–oxygen radial distribution function of liquid water determined by means of X-ray and neutron scattering measurements [43–46]. Consider, for instance, that the accessible surface area is usually calculated using a water probe radius of 1.40 Å [47].

The contact correlation function $G(R_c)$ determined by P&P for TIP4P water at 300 K is shown in Fig. 5 (empty squares), together with those calculated by means of SPT Eqs. (15) and (16): for $\sigma_1 = 2.70$ Å (solid line), $\sigma_1 = 2.75$ Å (dashed line), and $\sigma_1 = 2.80$ Å (dotted line). The pressure is always fixed at 1 atm. It is evident that the agreement is not good in all cases, even though, on increasing the size assigned to water molecules, the situation becomes slightly better. In particular, the experimental $G(R_c)$ shows a broad maximum of approximately 2.3 over the range 2.6 Å $\leq R_c \leq 3.0$ Å, whereas the SPT calculated functions show a significantly lower maximum at $R_c \approx 2.0$ Å. This deficiency of SPT could be related to the fact that it does not take into account the peculiar structural features of liquid water, as interpreted by P&P [12]. However, it has to be

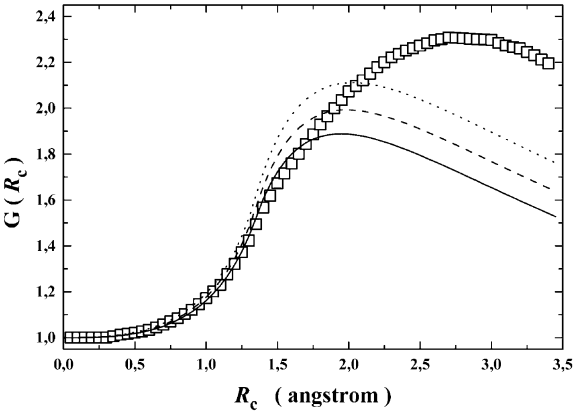


Fig. 5. Comparison between the contact correlation function for TIP4P water at 300 K (empty squares), determined by P&P [12], and those calculated using Eqs. (15) and (16) for $\sigma_1 =$ 2.70 Å (solid line), $\sigma_1 = 2.75$ Å (dashed line), and $\sigma_1 = 2.80$ Å (dotted line). The experimental density of water at 300 K is used in all cases.

noted that the contact correlation function of a Lennard–Jones liquid having the same number density and the same molecular size of liquid water, always determined by P&P [12], is only slightly different from that of TIP4P water (see Fig. 4 in [12]). This finding would suggest that: (a) the structure of the liquid is not so important in determining the $G(R_c)$ function; (b) the SPT deficiency is a simple consequence of the approximate character of the theory. It is worth noting that differences in $G(R_c)$ tend to be leveled down in calculating, by means of Eq. (9), the work of cavity creation (see below). Furthermore, the real physical significance of the maximum in $G(R_c)$ is not so clear, because it occurs at a cavity radius (less than the distance of closest approach between a water molecule and a methane molecule, $\approx 3.1$ Å) significantly smaller than that predicted for the crossover between small and large length scales by the Lum–Chandler–Weeks theory [40].

To emphasize the inadequacy of SPT to treat liquid water, P&P showed also that, for a cavity of $r_c = 2$ Å, SPT significantly underestimates the $\Delta G_c$ value exactly determined from computer simulations, approximately 27 kJ mol$^{-1}$ at 300 K [11]. This is true if $\sigma_1 = 2.70$ Å is used in Eq. (12). However, at 300 K for $\sigma_c = 4$ Å, the SPT

formula gives: $\Delta G_c$(in kJ mol$^{-1}$) = 22.1 for $\sigma_1$ = 2.70 Å, 24.1 for $\sigma_1$ = 2.75 Å, and 26.1 for $\sigma_1$ = 2.80 Å. These numbers indicate that: (a) SPT accounts for approximately 80% of the experimental $\Delta G_c$ value even when $\sigma_1$ = 2.70 Å is used; (b) with a very small increase in $\sigma_1$, from 2.70 to 2.80 Å, SPT is able to fully account for the experimental $\Delta G_c$ value. Since $\sigma_1$ = 2.80 Å is a physically sound size for water molecules, such values mean that SPT works satisfactory well even though H-bonds are not explicitly taken into account.

It is worth noting that Pratt and colleagues [17] found similar $\Delta G_c$ values in SPC water [48], a hard sphere liquid and a Lennard–Jones liquid, both constituted by spherical particles of the same size of water molecules and possessing the same number density of liquid water. The latter features, shared by the three liquids, should be the main determinants of the work of cavity creation. SPT uses as input data exactly the experimental density of liquid water and the hard sphere diameter assigned to water molecules [1,3,49,50].

Even the two-moment information theory approach recently developed by Pratt and colleagues [14–19] uses practically the same input data: the density of liquid water, and the oxygen–oxygen radial distribution function determined by means of computer simulations. In fact, even though the two-moment information theory approach does not assign a diameter to water molecules, the latter datum is built in through the oxygen–oxygen radial distribution function. The fact that 'the predicted thermodynamic results are surprisingly accurate when two moments are used but become worse with three moments, before eventually returning to an accurate prediction with many more moments available' is not 'fortuitous', as wrote by Pratt [21], but indicates, in our opinion, that the pair correlation function, not the higher-order ones, is important in determining cavity statistics in liquid water.

Furthermore, Garde and Ashbaugh [20] found that the work of cavity creation determined in an isotropic single-site model of water lacking the H-bonds, but retaining the same density and molecular size of water, is larger in magnitude than that determined in water models taking into full account the presence of H-bonds. This would suggest that a liquid characterized by the same density and the same molecular size of water but without H-bonds is more hydrophobic than real water, as already emerged from the simulations of Madan and Lee [23]. It has to be noted that, even though the model system of Garde and Ashbaugh has a pressure significantly higher than that of liquid water, this condition is strictly necessary to preserve the same number density of water. The latter is a fundamental requirement to make a meaningful comparison between cavity insertion probabilities in a water model with H-bonds turned on and in a water model with H-bonds turned off [see Eqs. (1)–(3)]. Therefore, H-bonds seem to be not really important in determining the magnitude of the work of cavity creation in water.

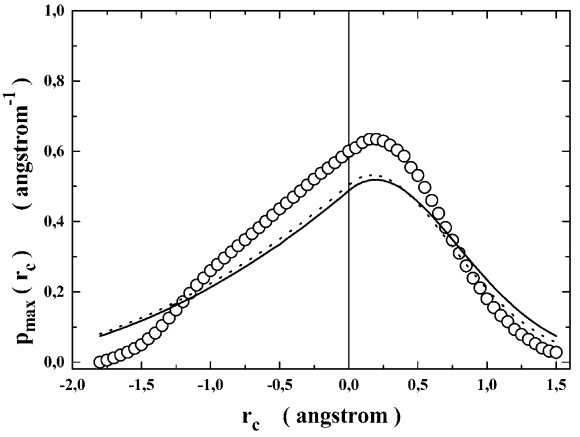


Fig. 6. Comparison between the 'experimental' cavity size distribution for *n*-hexane (empty circles), and those calculated using Eqs. (11) and (13) for $\sigma_1$ = 5.9 Å, and $P$ = 1 atm (solid line); and $\sigma_1$ = 6.0 Å and $P$ = 1 atm (dotted line). The experimental density of *n*-hexane at 320 K is used in both cases.

### 3.2. n-Hexane

The cavity size distribution functions calculated for *n*-hexane using Eqs. (11) and (13) are contrasted against the 'experimental' one determined by P&P for an OPLS model of *n*-hexane at 320 K from MD simulations in Figs. 6 and 7. Specifically: (a) the $P_{max}(r_c)$ functions calculated for $\sigma_1$ = 5.9 Å and $P$ = 1 atm (solid line), and $\sigma_1$ = 6.0 Å and

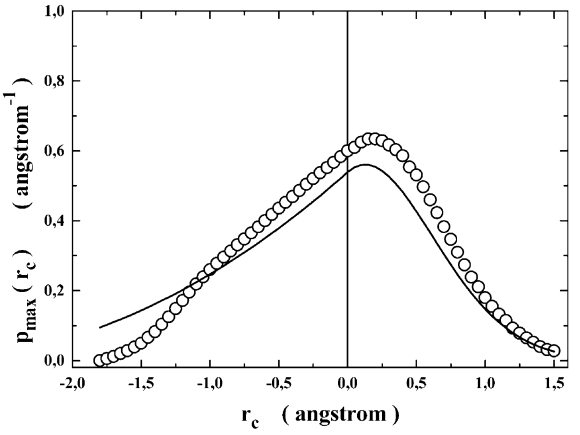


Fig. 7. Comparison between the 'experimental' cavity size distribution for *n*-hexane (empty circles), and that calculated using Eqs. (11) and (13) for $\sigma_1 = 6.2$ Å, $P = 1$ atm (solid line), and the experimental density of *n*-hexane at 320 K.

$P = 1$ atm (dotted line) are shown in Fig. 6; (b) the $P_{max}(r_c)$ function calculated for $\sigma_1 = 6.2$ Å and $P = 1$ atm (solid line) is shown in Fig. 7. In all cases the experimental molar volume of *n*-hexane at 320 K, 135 cm$^3$ mol$^{-1}$, is used [41]. For *n*-hexane, the $P_{max}(r_c)$ functions obtained by using $P$(SPT) in Eq. (13) are not shown because they are only slightly different from those obtained by using $P = 1$ atm.

The $P_{max}(r_c)$ functions calculated for $\sigma_1 = 5.9$ Å and 6.0 Å do not agree with the 'experimental' one over the whole cavity size range considered. That calculated for $\sigma_1 = 6.2$ Å does not agree with the 'experimental' one up to $r_c \approx 1.2$ Å, but the agreement becomes satisfactory on further increasing the cavity size. The results indicate that SPT is not able to reproduce the 'experimental' $P_{max}(r_c)$ function using the hard sphere diameter usually assigned to the *n*-hexane molecule, in the range 5.9–6.0 Å [51–54]. Such deficiency is strictly related to the fact that P&P considered a *n*-hexane molecule not as a single spherical exclusion volume, but, more realistically, as constituted by interpenetrating spherical methyl and methylene groups. This implies that SPT cannot reproduce the 'experimental' $P_{max}(r_c)$ function for small cavities (this is particularly striking for the region of negative $r_c$, where Eq. (11) should be exact, if $r_1$ would be the right one). The agreement should become better on increasing the cavity size since the *n*-hexane molecule should more resemble a single sphere. In fact, the agreement is good for molecular-sized cavities if $\sigma_1 = 6.2$ Å, a hard sphere diameter larger than the customary one. This implies that also the volume packing density of *n*-hexane is greater than the customary one obtained from hard sphere theories, as a consequence of the greater realism provided by computer simulations.

In fact, Wodak and co-workers reported $\Delta G_c \cong 20$ kJ mol$^{-1}$ at 300 K to create a cavity of $r_c = 2$ Å in liquid *n*-hexane [53]. The SPT formula, Eq. (12), at 300 K for $\sigma_c = 4$ Å, gives 14.8 kJ mol$^{-1}$ if $\sigma_1 = 5.9$ Å, and 21.0 kJ mol$^{-1}$ if $\sigma_1 = 6.2$ Å. These numbers confirm that SPT compare favorably with computer simulation results for molecular-sized cavities if the hard sphere diameter of *n*-hexane molecules is fixed at 6.2 Å. Therefore, the SPT results seem to have consistency.

Finally, to further point out the effect of explicitly considering the methyl and methylene groups, we calculated $P_{max}(r_c)$ for $\sigma_1 = 4.9$ Å and $v_1 = 80$ cm$^3$ mol$^{-1}$. In this manner the agreement with the 'experimental' function is satisfactory over the whole region of positive $r_c$, as shown in Fig. 8. Clearly, the values of the hard sphere diameter and

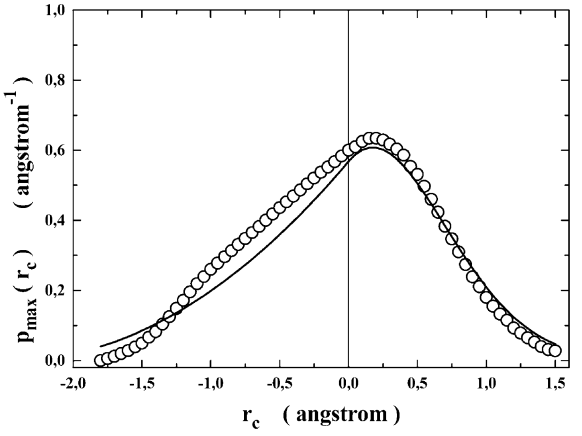


Fig. 8. Comparison between the 'experimental' cavity size distribution for *n*-hexane (empty circles), and that calculated using Eqs. (11) and (13) for $\sigma_1 = 4.9$ Å, $P = 1$ atm (solid line), and $v_1 = 80$ cm$^3$·mol$^{-1}$ at 320 K.

molar volume used in this case are unreliable. The example serves only to show that the number density of *n*-hexane seems to be higher by explicitly considering the methyl and methylene groups constituting a *n*-hexane molecule in computer simulations. This is confirmed by the fact that the $P_{max}(r_c)$ distribution determined by P&P for *n*-dodecane is superimposable to that of *n*-hexane [12].

## 4. Discussion

The motivation of the present investigation is perfectly clarified by the following Pratt's statements [21]: 'Conventional molecular simulation calculations with widely accepted molecular interaction models for small hydrophobic species in water broadly agree with experimental results on such systems. In this sense, everything is known. Nevertheless, this complete knowledge hasn't achieved a consensus for a primitive mechanism of hydrophobic effects. By 'mechanism' we mean here a simpler, physical description that ties together otherwise disparate observations. The elementary simplifications that lead to a mechanism must be more than rationalizations; they must be verifiable and consistent at a more basic level of theory, calculation, and observation.'

The reference system for liquids is the hard sphere fluid and it has been shown that the SPT analytical expressions accurately reproduce the Monte Carlo simulation results of the work of cavity creation and cavity size distribution in hard sphere fluids spanning the entire fluid density range [55]. In addition, the development and application of SPT by Reiss and colleagues, pointed out that molecular liquids are apparently similar in some important respects to hard sphere fluids [2,30]. The attractive part of the intermolecular potential determines the liquid density; once the density is fixed, the liquid can be regarded as an assembly of hard spheres confined within a defined volume and can be treated by SPT. The same view emerged from the famous Weeks–Chandler–Andersen theory [25].

Thus, it should be important to verify if SPT would be able to reproduce the 'experimental' $P_{max}(r_c)$ distributions determined by P&P, using in SPT equations the experimental values for the density and molecular size of the liquid solvent. Clearly, the agreement between the SPT results and the P&P cavity size distributions cannot be straightforward because the size of molecules is an ill-defined quantity for polyatomic molecules, a feature of all common solvents. It proves that a satisfactory agreement can be reached in the case of water over the whole cavity size range considered, whereas in the case of *n*-hexane only for molecular-sized cavities, by a proper choice of the solvent molecule diameter.

de Souza and Ben-Amotz [56], using expressions derived from the Carnahan–Starling equation of state [57], were able to obtain good agreement for both water and *n*-hexane over the whole range of positive $r_c$, using $\sigma_1 = 2.56$ Å for water, and $\sigma_1 = 6.12$ Å for *n*-hexane. Actually, we do not understand what is the cause of the marked difference with our SPT results.

The fact that SPT works better for water than for *n*-hexane may appear strange at first sight [12,58]. However, it is readily rationalized by considering: (a) the importance that molecular structure (i.e. the connectivity of groups in a molecule) plays on the partitioning of empty space, especially when very small cavities are considered; (b) the circumstance that it is more reliable to consider as a single spherical exclusion volume a water molecule than an *n*-hexane molecule.

In any case, it is important to underscore that: (a) SPT is able to predict that the $P_{max}(r_c)$ distribution is narrower for water than for *n*-hexane; (b) by a proper choice of the size of water molecules (i.e. the size value selected by P&P for very small interstitial holes, $\sigma_1 = 2.70$ Å, and a physically sound size for molecular-sized cavities, $\sigma_1 = 2.80$ Å), the SPT results agree with the 'experimental' ones. The obvious criticism is that the choice of the size of solvent molecules to be used in SPT formulas is a heuristic procedure to reach agreement. The reply is that $\sigma_1 = 2.80$ Å cannot be considered a heuristic diameter for water molecules in view of the available oxygen-oxygen radial distribution functions of water (i.e. the distance between two H-bonded water molecules is approximately 2.80 Å [43–46]). Furthermore, as well emphasized by Fig. 2, the $P_{max}(r_c)$ calcu-

lated with $\sigma_1 = 2.70$ Å is close to the 'experimental' one. In this respect it is worth noting that: (a) all the theoretical approaches to hydrophobic hydration use information on the size of water molecules; (b) SPT has provided various means to determine the size of solvent molecules and their temperature dependence (the procedure of analyzing gas solubility data, originally devised by Pierotti [33,34], and fruitfully exploited by Wilhelm and Battino [51], has proven to be very effective). Since SPT does not explicitly take into account the presence of H-bonds, its success would imply that the size of water molecules is the main factor in determining the cavity size distribution in water.

This interpretation contrasts with the view lucidly expressed by Pratt [21]: 'What was decidedly different between water and organic solvents was the flexibility of the medium to open cavities larger than the most probable size. Water is less flexible in this regard, stiffer on a molecular scale, than typical organic liquids.' Pratt and colleagues [15,19] suggest that a clear indication of such stiffness is provided by the numerical values of the isothermal compressibility $\beta_T$ for the various solvents. In fact, $\beta_T$ for water is significantly smaller than for common organic solvents, and has a significantly smaller temperature dependence [15,59]. This answer, however, is unsatisfactory, because $\beta_T$ is a macroscopic thermodynamic quantity and one, in turn, should provide a molecular explanation of its abnormality in the case of water. Moreover, it has to be noted that $\beta_T$ does not enter into the formulas used to calculate $P_0$ and so $\Delta G_c$, even in the two-moment information theory model [14,15]. It was the assumption of a continuous Gaussian distribution for the occupancy number that led to the appearance of $\beta_T$ into the formulas [15,60]. However, the assumption of a Gaussian probability functional for the density field has no firm theoretical grounds and is not supported by computer simulation results [20,61]. Some pitfalls of the Gaussian model were directly discussed by Pratt and colleagues [15].

On the same line, there is not a clear and logic connection between the stiffness of water and the large entropy loss characteristic of hydrophobic hydration around room temperature, because structure enhancement and orientational order increase of water molecules constituting the hydration shell of non-polar solutes 'are not direct features of this qualitative perspective' [62].

In addition, the statement 'hydrophobic effects can be attributed in large part to the equation of state for pure water' [63] cannot be considered a satisfactory answer for the simple mechanism invoked by Pratt. In fact, the cavity size distribution is a property of pure water and must be governed by the equation of state of pure water like any other property of pure water. This is self-evident: one does not need any sophisticated calculations to know that. The equation of state contains all necessary information, but it may contain more than what is needed to determine the cavity size distribution and so the work of cavity creation. The real question is whether the density of water and the size of water molecules are enough or not. As well emphasized by the van der Waals equation of state, two molecular features mainly determine the equation of state of a liquid: the size of the molecules and the strength of their attractive interactions. Clearly, the H-bonds play a fundamental role in determining the density of liquid water, together with the small molecular size (note that the number density of water is approximately one order of magnitude greater than that of common organic solvents). However, both the results of computer simulations and the application of SPT indicate that, when the density is established, the smallness of water molecules is the factor controlling the probability of cavity occurrence.

In conclusion we think that each reader, on the basis of the material presented in this work, may select between the two interpretations.

## Acknowledgments

Work supported by grants from the Italian Ministry for Instruction, University, and Research (M.I.U.R., Rome).

## References

[1] B. Lee, The physical origin of the low solubility of non-polar solutes in water, Biopolymers 24 (1985) 813–823.

[2] H. Reiss, Scaled particle methods in the statistical thermodynamics of fluids, Adv. Chem. Phys. 9 (1966) 1–84.
[3] R.A. Pierotti, A scaled particle theory of aqueous and non-aqueous solutions, Chem. Rev. 76 (1976) 717–726.
[4] B. Lee, Solvent reorganization contribution to the transfer thermodynamics of small non-polar molecules, Biopolymers 31 (1991) 993–1008.
[5] M. Lucas, Size effect in transfer of non-polar solutes from gas or solvent to another solvent with a view on hydrophobic behavior, J. Phys. Chem. 80 (1976) 359–362.
[6] K. Soda, Solvent exclusion effect predicted by the scaled particle theory as an important factor of the hydrophobic effect, J. Phys. Soc. J. 62 (1993) 1782–1793.
[7] A. Wallqvist, D.G. Covell, On the origins of the hydrophobic effect: observations from simulations of *n*-dodecane in model solvents, Biophys. J. 71 (1996) 600–608.
[8] M. Ikeguchi, S. Shimizu, S. Nakamura, K. Shimizu, Roles of hydrogen bonding and the hard core of water on hydrophobic hydration, J. Phys. Chem. Part B 102 (1998) 5891–5898.
[9] E. Gallicchio, M.M. Kubo, R.M. Levy, Enthalpy-entropy and cavity decomposition of alkane hydration free energies: numerical results and implications for theories of hydrophobic solvation, J. Phys. Chem. Part B 104 (2000) 6271–6285.
[10] G. Graziano, Size dependence of the solubility of non-polar compounds in different solvents, Can. J. Chem. 80 (2002) 401–412.
[11] A. Pohorille, L.R. Pratt, Cavities in molecular liquids and the theory of hydrophobic solubilities, J. Am. Chem. Soc. 112 (1990) 5066–5074.
[12] L.R. Pratt, A. Pohorille, Theory of hydophobicity: transient cavities in molecular liquids, Proc. Natl. Acad. Sci. USA 89 (1992) 2995–2999.
[13] L.R. Pratt, A. Pohorille, in: M.U. Palma, M.B. Palma-Vittorelli, F. Parak (Eds.), Water-biomolecule interactions, Hydrophobic effects from cavity statistics, Società Italiana di Fisica, Bologna, 1993, pp. 261–268.
[14] G. Hummer, S. Garde, A.E. Garcia, A. Pohorille, L.R. Pratt, An information theory model of hydrophobic interactions, Proc. Natl. Acad. Sci. USA 93 (1996) 8951–8955.
[15] G. Hummer, S. Garde, A.E. Garcia, M.E. Paulaitis, L.R. Pratt, Hydrophobic effects on a molecular scale, J. Phys. Chem. Part B 102 (1998) 10469–10482.
[16] A. Pohorille, Transient cavities in liquids and the nature of the hydrophobic effect, Pol. J. Chem. 72 (1998) 1680–1690.
[17] M.A. Gomez, L.R. Pratt, G. Hummer, S. Garde, Molecular realism in default models for information theories of hydrophobic effects, J. Phys. Chem. Part B 103 (1999) 3520–3523.
[18] L.R. Pratt, G. Hummer, S. Garde, in: C. Caccamo, J.P. Hansen, G. Stell (Eds.), New approaches to problems in liquid state theory, Theories of hydrophobic effects and the description of free volume in complex liquids, NATO Science Series 529, Kluwer, The Netherlands, 1999, pp. 407–420.
[19] G. Hummer, S. Garde, A.E. Garcia, L.R. Pratt, New perspectives on hydrophobic effects, Chem. Phys. 258 (2000) 349–370.
[20] S. Garde, H.S. Ashbaugh, Temperature dependence of hydrophobic hydration and entropy convergence in an isotropic model of water, J. Chem. Phys. 115 (2001) 977–982.
[21] L.R. Pratt, Molecular theory of hydrophobic effects: 'She is too mean to have her name repeated, Annu. Rev. Phys. Chem. 53 (2002) 409–436.
[22] X. Siebert, G. Hummer, Hydrophobicity maps of the *N*-peptide coiled coil of HIV-1 gp41, Biochemistry 41 (2002) 2956–2961.
[23] B. Madan, B. Lee, Role of hydrogen bonds in hydrophobicity: the free energy of cavity formation in water models with and without the hydrogen bonds, Biophys. Chem. 51 (1994) 279–289.
[24] S. Chandrasekhar, Stochastic problems in physics and astronomy, Rev. Mod. Phys. 15 (1943) 1–89.
[25] D. Chandler, J.D. Weeks, H.C. Andersen, van der Waals picture of liquids, solids and phase-transformations, Science 220 (1983) 787–794.
[26] R.C. Tolman, The principles of statistical mechanics, Oxford University Press, London, 1938, pp. 636–641.
[27] B. Lee, A procedure for calculating thermodynamic functions of cavity formation from the pure solvent simulation data, J. Chem. Phys. 83 (1985) 2421–2425.
[28] H. Reiss, Statistical geometry in the study of fluids and porous media, J. Phys. Chem. 96 (1992) 4736–4747.
[29] H. Reiss, H.L. Frisch, J.L. Lebowitz, Statistical mechanics of rigid spheres, J. Chem. Phys. 31 (1959) 369–380.
[30] H. Reiss, R.V. Casberg, Radial distribution function for hard spheres from scaled particle theory, and an improved equation of state, J. Chem. Phys. 61 (1974) 1107–1114.
[31] W.L. Jorgensen, J. Chandrasekhar, J.D. Madura, R.W. Impey, M.L. Klein, Comparison of simple potential functions for simulating liquid water, J. Chem. Phys. 79 (1983) 926–935.
[32] W.L. Jorgensen, J.D. Madura, C.J. Swenson, Optimized intermolecular potential functions for liquid hydrocarbons, J. Am. Chem. Soc. 106 (1984) 6638–6646.
[33] R.A. Pierotti, The solubility of gases in liquids, J. Phys. Chem. 67 (1963) 1840–1845.
[34] R.A. Pierotti, Aqueous solutions of non-polar gases, J. Phys. Chem. 69 (1965) 281–288.
[35] A. Ben-Naim, H.L. Friedman, On the application of the scaled particle theory to aqueous solutions of non-polar gases, J. Phys. Chem. 71 (1967) 448–449.
[36] F.H. Stillinger, Structure in aqueous solutions of non-polar solutes from the standpoint of scaled-particle theory, J. Solution Chem. 2 (1973) 141–158.

[37] R.A. Pierotti, On the scaled-particle theory of dilute aqueous solutions, J. Phys. Chem. 71 (1967) 2366–2367.
[38] H.S. Ashbaugh, M.E. Paulaitis, Effect of solute size and solute-water attractive interactions on hydration water structure around hydrophobic solutes, J. Am. Chem. Soc. 123 (2001) 10721–10728.
[39] J.R. Henderson, Solvation of a solvophobic sphere, J. Chem. Phys. 116 (2002) 5039–5045.
[40] K. Lum, D. Chandler, J.D. Weeks, Hydrophobicity at small and large length scales, J. Phys. Chem. Part B 103 (1999) 4570–4577.
[41] D.R. Lide (Ed.), Handbook of chemistry and physics, 77th edition, CRC Press, Boca Raton, FL, 1996.
[42] S. Shimizu, M. Ikeguchi, S. Nakamura, K. Shimizu, Size dependence of transfer free energies: a hard-sphere-chain-based formalism, J. Chem. Phys. 110 (1999) 2971–2982.
[43] A.H. Narten, H.A. Levy, Observed diffraction pattern and proposed models of liquid water, Science 165 (1969) 447–454.
[44] A.K. Soper, F. Bruni, M.A. Ricci, Site-site pair correlation functions of water from 25 to 400 °C: revised analysis of new and old diffraction data, J. Chem. Phys. 106 (1997) 247–254.
[45] J.M. Sorenson, G. Hura, R.M. Glaeser, T. Head-Gordon, What can X-ray scattering tell us about the radial distribution functions of water?, J. Chem. Phys. 113 (2000) 9149–9161.
[46] G. Hura, T. Head-Gordon, Water structure from scattering experiments and simulation, Chem. Rev. 102 (2002) 2651–2670.
[47] B. Lee, F.M. Richards, The interpretation of protein structures: estimation of static accessibility, J. Mol. Biol. 55 (1971) 379–400.
[48] H.J.C. Berendsen, W.F. van Gunsteren, J.P.M. Postma, J. Hermans, in: B. Pullman (Ed.), Intermolecular forces, Interaction models for water in relation to protein hydration, Reidel, Dordrecht, 1981, pp. 331–342.
[49] M. Kodaka, Reevaluation in interpretation of hydrophobicity by scaled particle theory, J. Phys. Chem. B 105 (2001) 5592–5594.
[50] G. Graziano, Comment on reevaluation in interpretation of hydrophobicity by scaled particle theory, J. Phys. Chem. Part B 106 (2002) 7713–7716.
[51] E. Wilhelm, R. Battino, Estimation of Lennard–Jones (6,12) pair potential parameters from gas solubility data, J. Chem. Phys. 55 (1971) 4012–4017.
[52] D. Ben-Amotz, K.G. Willis, Molecular hard-sphere volume increments, J. Phys. Chem. 97 (1993) 7736–7742.
[53] M. Prevost, I. Tomàs-Oliveira, J.P. Kocher, S.J. Wodak, Free energy of cavity formation in liquid water and hexane, J. Phys. Chem. 100 (1996) 2738–2743.
[54] J.P. Kocher, M. Prevost, S.J. Wodak, B. Lee, Properties of the protein matrix revealed by the free energy of cavity formation, Structure 4 (1996) 1517–1529.
[55] L.E.S. de Souza, A. Stamatopoulou, D. Ben-Amotz, Chemical potentials of hard sphere solutes in hard sphere solvents. Monte Carlo simulations and analytical approximations, J. Chem. Phys. 100 (1994) 1456–1459.
[56] L.E.S. de Souza, D. Ben-Amotz, Hard fluid model for molecular solvation free energies, J. Chem. Phys. 101 (1994) 9858–9863.
[57] G.A. Mansoori, N.F. Carnahan, K.E. Starling, T.W. Leland, Equilibrium thermodynamic properties of the mixture of hard spheres, J. Chem. Phys. 54 (1971) 1523–1525.
[58] I. Tomàs-Oliveira, S.J. Wodak, Thermodynamics of cavity formation in water and *n*-hexane using Widom particle insertion method, J. Chem. Phys. 111 (1999) 8576–8587.
[59] J.S. Rowlinson, F.L. Swinton, Liquids and liquid mixtures, Butterworths, London, 1982.
[60] S. Garde, G. Hummer, A.E. Garcia, M.E. Paulaitis, L.R. Pratt, Origin of entropy convergence in hydrophobic hydration and protein folding, Phys. Rev. Lett. 77 (1996) 4966–4968.
[61] D.M. Huang, D. Chandler, Cavity formation and the drying transition in the Lennard–Jones fluid, Phys. Rev. E 61 (2000) 1501–1506.
[62] L.R. Pratt, A. Pohorille, Hydrophobic effects and modeling of biophysical aqueous solution interfaces, Chem. Rev. 102 (2002) 2671–2692.
[63] H.S. Ashbaugh, T.M. Truskett, P.G. Debenedetti, A simple molecular thermodynamic theory of hydrophobic hydration, J. Chem. Phys. 116 (2002) 2907–2921.